Pattern formation of a predator-prey system with Ivlev-type functional response

Weiming Wang [a,*], Lei Zhang [a,b], Hailing Wang [c] Zhenqing Li [d]

[a] Institute of Nonlinear Analysis, School of Mathematics and Information Science, Wenzhou University, Wenzhou, 325035 P.R. China

[b] Department of Mathematics, North University of China, Taiyuan, Shan'xi 030051

[c] College of Computer Science and Technology, Chongqing University of Posts and Telecommunications, Chongqing 400065

[d] Laboratory of Quantitative Vegetation Ecology, Institute of Botany, The Chinese Academy of Sciences, Beijing 100093

Abstract

In this paper, we investigate the emergence of a predator-prey system with Ivlev-type functional response and reaction-diffusion. We study how diffusion affects the stability of predator-prey coexistence equilibrium and derive the conditions for Hopf and Turing bifurcation in the spatial domain. Based on the bifurcation analysis, we give the spatial pattern formation, the evolution process of the system near the coexistence equilibrium point, via numerical simulation. We find that pure Hopf instability leads to the formation of spiral patterns and pure Turing instability destroys the spiral pattern and leads to the formation of chaotic spatial pattern. Furthermore, we perform three categories of initial perturbations which predators are introduced in a small domain to the coexistence equilibrium point to illustrate the emergence of spatiotemporal patterns, we also find that in the beginning of evolution of the spatial pattern, the special initial conditions have an effect on the formation of spatial patterns, though the effect is less and less with the more and more iterations. This indicates that for prey-dependent type predator-prey model, pattern formations do depend on the initial conditions, while for predator-dependent type they do not. Our results show that modeling by reaction-diffusion equations is an appropriate tool for investigating fundamental mechanisms of complex spatiotemporal dynamics.

Key words: Hopf bifurcation; Turing instability; Spatiotemporal pattern; Spiral wave

* Corresponding author.
Email address: `weimingwang2003@163.com.` (Weiming Wang).

1 Introduction

A fundamental goal of theoretical ecology is to understand how the interactions of individual organisms with each other and with the environment determine the distribution of populations and the structure of communities. Empirical evidence suggests that the spatial scale and structure of environment can influence population interactions(Cantrell & Cosner, 2003). The endless array of patterns and shapes in nature has long been a source of joy and wonder to laymen and scientists alike. Discovering how such patterns emerge spontaneously from an orderless and homogeneous environment has been a challenge to researchers in the natural sciences throughout the ages (Ben-Jacob & Levine, 2001). The problem of pattern and scale is the central problem in ecology, unifying population biology and ecosystems science, and marrying basic and applied ecology (Levin, 1992). The study of spatial patterns in the distribution of organisms is a central issue in ecology (Levin, 1992; Koch & Meinhardt, 1994; Neuhauser, 2001; Alonso, Bartumeus & Catalan, 2002; Medvinsky et al, 2002; Cantrell & Cosner, 2003; Leppänen et al, 2003; Leppänen, 2004; Murray, 2003; Hawick, James & Scogings, 2006; Griffith & Peres-Netob, 2006; Maini, Baker, Chuong, 2006; Pearce et al, 2006; Baurmann, Gross, & Feudel, 2007; Liu & Jin, 2007; Schnell, Grima & Maini, 2007; Shoji, Yamada, Ueyama & Ohta, 2007; Wang, Liu & Jin, 2007) since the pioneering work of Alan Turing (Tuing, 1952). And Turing reaction-diffusion system explains spatial patterns spontaneously forming in a perfectly homogeneous field (Uriu & Iwasa, 2007). The instability now identified with Turing's name is believed to be involved in the formation of structure in many systems of biological interest (Murray, 2003). Theoretical work has shown that spatial and temporal pattern formation can play a very important role in ecological and evolutionary systems. Patterns can affect, for example, stability of ecosystems, the coexistence of species, invasion of mutants and chaos. Moreover, the patterns themselves may interact, leading to selection on the level of patterns, interlocking ecoevolutionary time scales, evolutionary stagnation and diversity (Savill & Hogeweg, 1999).

The origin of these patterns has commonly attributed to two sorts of sources (Levin, 1992). One is a heterogeneous distribution of abiotic factors and the other is underlying mechanisms at the level of individuals. Patterns generated in abiotically homogeneous environments are particularly interesting because they require an explanation based on the individual behavior of organisms. They are commonly called "emergent patterns", because they emerge from interactions in spatial scales that are much larger than the characteristic scale of individuals (Alonso, Bartumeus & Catalan, 2002). The instability leads to a process that might be called differentiation and in its simplest realization is the result of a competition between an activator (for predator-prey system, prey) and an inhibitor (for predator-prey system, predator) diffusing at different rates. The results of the instability has one characteristic property: its scale

or wavelength is determined by the concentrations of ambient species and the diffusion coefficients, and is therefore independent of any externally imposed length scales. In the process of morphogenesis the instability is likely to be triggered by the increasing scale of the system: the instability occurs once the system is large enough that it contains several natural wavelengths of the instability (Callahan & Knobloch, 1999).

The past investigations have revealed that spatial inhomogeneities like the inhomogeneous distribution of nutrients as well as interactions on spatial scales like migration can have an important impact on the dynamics of ecological populations (Medvinsky et al, 2002; Murray, 2003). In particular it has been shown that spatial inhomogeneities promote the persistence of ecological populations, play an important role in speciation and stabilize population levels (Baurmann, Gross, & Feudel, 2007). Spatial ecology today is still dominated by theoretical investigations, and empirical studies that explore the role of space are becoming more common due to technological advances that allow the recording of exact spatial locations (Neuhauser, 2001).

On the other hand, as we know, our ecological environment is a huge and highly complex system. This complexity arises in part from the diversity of biological species, and also from the complexity of every individual organism (Jost, 1998). The relationship between predators and their prey has long been and will continue to be one of dominant themes in both ecology and mathematical ecology due to its universal existence and importance (Kuang & Beretta, 1998). A classical predator-prey system can be written as the form (Abram & Ginzburg, 2000; Alonso, Bartumeus & Catalan, 2002):

$$\dot{u} = uf(u) - vg(u,v), \qquad \dot{v} = h[g(u,v),v]v. \tag{1}$$

where u and v are prey and predator density, respectively, $f(u)$ the prey growth rate, $g(u,v)$ the functional response, the prey consumption rate by an average single predator, which obviously increases with the prey consumption rate, and can be influenced by the predator density, $h[g(u,v),v]$ the per capita growth rate of predators (also known as the "predator numerical response"). The most widely accepted assumption for the numerical response is the linear one (Arditi & Ginzburg, 1989; Alonso, Bartumeus & Catalan, 2002):

$$h[g(u,v),v] = \varepsilon g(u,v) - \beta,$$

where β is a per capita predator death rate and ε the conversion efficiency of food into offsprings.

In population dynamics, a functional response $g(u,v)$ of the predator to the prey density refers to the change in the density of prey attached per unit time per predator as the prey density changes (Ruan & Xiao, 2001). In general, functional response can be classified as (i) prey dependent, when prey density

alone determines the response, $g(u,v) = p(N)$; (ii) predator dependent, when both predator and prey populations affect the response. Particularly, when $g(u,v) = p(\frac{u}{v})$, we call model (1) strictly ratio dependent; and (iii) multi-species dependent, when species other than the focal predator and its prey species influence the functional response (Abram & Ginzburg, 2000).

There have been several famous functional response types: Holling type I–III (Holling, 1959a,b); Hassell-Varley type (Hassell & Varley, 1969); Beddington-DeAngelis type by Beddington (Beddington, 1975) and DeAngelis, Goldstein and Neill (DeAngelis, Goldstein & Neill, 1975) independently; the Crowley-Martin type (Crowley & Martin, 1989); and the recent well-known ratio-dependence type by Arditi and Ginzburg (Arditi & Ginzburg, 1989) later studied by Kuang and Beretta (Kuang & Beretta, 1998). Of them, the Holling type I—III was labeled "prey-dependent" and the other types that consider the interference among predators were labeled "predator-dependent" (Arditi & Ginzburg, 1989).

Besides Holling type I–III, there is another important prey-dependent functional response–Ivlev-type, originally due to Ivlev (Ivlev, 1961):

$$g(u,v) = 1 - e^{-\gamma u}. \tag{2}$$

and the corresponding Ivlev-type predator-prey model takes the form:

$$\dot{u} = u(1-u) - v(1 - e^{-\gamma u}), \qquad \dot{v} = \varepsilon v(1 - e^{-\gamma u}) - \beta v. \tag{3}$$

where u and v represent population density of prey and predator at time t, respectively, ε, β, γ are positive constants, ε the conversion rate of prey captured by predator, β the deathrate of predator, and γ the efficiency of predator capture of prey. From an ecological viewpoint, the conditions $\dot{u} > 0$ and $\dot{v} > 0$ must hold. From the second equation of (3), we know $\varepsilon > \beta$.

In this paper, we mainly focus on the following spatial Ivlev-type predator-prey model with reaction diffusion:

$$\begin{aligned}
\dot{u} &= \overbrace{u(1-u)}^{\text{growth due to prey}} - \overbrace{v(1-e^{-\gamma u})}^{\text{mortality due to prey}} + \overbrace{d_1 \nabla^2 u}^{\text{random motility}} \equiv f(u,v) + d_1 \nabla^2 u, \\
\dot{v} &= \underbrace{\alpha\beta v(1-e^{-\gamma u})}_{\text{growth due to predator}} - \underbrace{\beta v}_{\text{mortality due to predator}} + \underbrace{d_2 \nabla^2 v}_{\text{random motility}} \\
&\equiv g(u,v) + d_2 \nabla^2 v.
\end{aligned} \tag{4}$$

where $\alpha = \frac{\varepsilon}{\beta} > 1$, and d_1, d_2 are the diffusion coefficients of prey and predator, respectively, $\nabla^2 = \frac{\partial}{\partial x^2} + \frac{\partial}{\partial y^2}$ is the usual Laplacian operator in two-dimensional space.

Both ecologists and mathematicians are interested in the Ivlev-type predator-prey model and much progress has been seen in the study of model (3) (May, 1981; Metz & Diekmann, 1986; Kooij, 1996; Sugie, 1998; Tian, 2006; Wang, 2007; Preedy et al., 2006) and model (4) (Sherratt, Lewis & Fowler, 1995; Sherratt, Eagan & Lewis, 1997; Kay & Sherratt, 2000; Pearce et al, 2006; Garvie, 2007; Preedy et al., 2006; Uriu & Iwasa, 2007). The results indicate that the Ivlev-type predator-prey model (3) and (4) have widely applicabilities in ecology, such as dynamics in predator-prey system (May, 1981; Metz & Diekmann, 1986; Sherratt, Lewis & Fowler, 1995; Sherratt, Eagan & Lewis, 1997; Tian, 2006), host-parasitoid system (Pearce et al, 2006; Preedy et al., 2006), fish skin pattern (Uriu & Iwasa, 2007), and so on.

Of them, Sherratt and co-workers had studied the dynamics of oscillations and chaos behind predator-prey invasion (Sherratt, Lewis & Fowler, 1995; Sherratt, Eagan & Lewis, 1997). Especially, in reference (Sherratt, Eagan & Lewis, 1997), the authors performed a large number of numerical simulations of the invasion of prey by predator with four categories models, involving one- and two-dimensional reaction-diffusion model (4). For model (4), they used a large spatial domain, with the system initially in the prey-only steady state, except for a small region in the center of the domain, where a small density of predators was introduced. They stopped their simulations before the invading wave reached the end of the domain, so that the results were not sensitive to the boundary conditions, which could be either zero flux, periodic, or with population levels fixed at the prey-only steady state. They also discussed the way in which the populations evolved after the invasion had reached the edge of the domain. Furthermore, the authors performed a number of one-dimensional spatial patterns with the model (4) initially in the prey-only steady state and two-dimensional spatial patterns with two categories of initial perturbation. One is the introduction of predators are in a small, localized region of the domain, which is otherwise in the prey-only steady state; the other is the introduction of predators along a line running parallel to one edge of the (rectangular) spatial domain. Based on these results, the authors indicated that for model (4), the behavior behind the invasive front of predators consists of either irregular spatiotemporal oscillations, or periodic waves in population density.

But to our knowledge, for model (4), the research on symbolic conditions of Hopf and Turing bifurcation, the evolution process of the spatial pattern formation, the mechanism of pattern formation emergence, especially the influences of the specific choice of the initial conditions to the pattern formation, seems rare.

The paper is organized as follows: In Section 2, we employ the method of stability analysis to derive the symbolic conditions for Hopf and Turing bifurcation in the spatial domain. Based on these conditions we locate the Hopf and Turing bifurcation within the generalized parameter domain in $\gamma - d_1$

bifurcation diagram. In Section 3, we give the spatial pattern formation, the evolution process of the system near the coexistence equilibrium point, via numerical simulation. For the sake of learning the influences of the initial conditions to pattern formation, we perform three categories of initial perturbations which predators are introduced in a small, localized region of the circle, line and pitchfork domain to the coexistence equilibrium point to illustrate the emergence of spatiotemporal patterns. Then, in the last section, we give some discussions and remarks.

2 Stability and Bifurcation analysis

The non-spatial model (3) has at most three equilibria (stationary states), which correspond to spatially homogeneous equilibria of the model (4), in the positive quadrant:

(i) (0, 0) (total extinct) is a saddle point;

(ii) $(1, 0)$ (extinct of the predator, or prey-only) is a saddle when $\gamma > -\ln\frac{\alpha-1}{\alpha}$, or stable node when $\gamma < -\ln\frac{\alpha-1}{\alpha}$, or saddle-node when $\gamma = -\ln\frac{\alpha-1}{\alpha}$;

(iii) a nontrivial stationary state (u^*, v^*) (coexistence of prey and predator), where

$$u^* = -\tfrac{1}{\gamma}\ln\left(\tfrac{\alpha-1}{\alpha}\right), \qquad v^* = -\tfrac{\alpha}{\gamma^2}\ln\left(\tfrac{\alpha-1}{\alpha}\right)\left(\gamma + \ln(\tfrac{\alpha-1}{\alpha})\right) = \tfrac{u^*(1-u^*)}{1-e^{-\gamma u^*}}. \quad (5)$$

with $\alpha > 1,\ \gamma > -\ln\left(\frac{\alpha-1}{\alpha}\right)$.

In this paper, we mainly focus on the dynamics of nontrivial stationary state (u^*, v^*). For cyclical populations, this coexistence state will also be unstable and will lie inside a stable limit cycle in the kinetic phase plane.

To perform a linear stability analysis, we linearize the dynamic system (4) around the spatially homogenous fixed point (5) for small space- and time-dependent fluctuations and expand them in Fourier space

$$u(\vec{x}, t) \sim u^* e^{\lambda t} e^{i\vec{k}\cdot\vec{x}}, \quad v(\vec{x}, t) \sim v^* e^{\lambda t} e^{i\vec{k}\cdot\vec{x}}.$$

Then, in the linearized version of model (4), yielding a dispersion relation from which one can choose parameters to allow only some of the modes with $\mathrm{Re}(\lambda) > 0$ to grow in time. The dispersion relation $\lambda(k)$ relating the temporal growth rate to the spatial wave number k can be found from the characteristic

polynomial of the original problem (4):

$$\lambda^2 - \mathrm{tr}_k \lambda + \Delta_k = 0, \tag{6}$$

where

$$\mathrm{tr}_k = f_u + g_v - k^2(d_1 + d_2) \equiv \mathrm{tr}_0 - k^2(d_1 + d_2),$$

$$\Delta_k = f_u g_v - f_v g_u - k^2(f_u d_2 + g_v d_1) + k^4 d_1 d_2 \equiv \Delta_0 - k^2(f_n d_2 + g_p d_1) + k^4 d_1 d_2,$$

here $\mathrm{tr}_0 = f_u + g_v$, $\Delta_0 = f_u g_v - f_v g_u$, and the elements f_u, f_v, g_u, g_v are the partial derivatives of the reaction kinetics $f(u, v)$ and $g(u, v)$ denoted by (4), evaluated at the stationary state (u^*, v^*).

The reaction-diffusion systems have led to the characterization of two basic types of symmetry-breaking bifurcations—Hopf and Turing bifurcation, responsible for the emergence of spatiotemporal patterns. See, for details, references (Yang et al, 2002; Wang, Liu & Jin, 2007).

The Hopf bifurcation occurs when $\mathrm{Im}(\lambda(k)) \neq 0$ and $\mathrm{Re}(\lambda(k)) = 0$ at $k = 0$, and the critical value of Hopf bifurcation parameter γ equals

$$\gamma_H = \frac{A(2 + A)}{(1 - \alpha)(1 + A)}, \tag{7}$$

where $A = (\alpha - 1) \ln \frac{\alpha - 1}{\alpha}$.

At the Hopf bifurcation threshold, the temporal symmetry of the system is broken and gives rise to uniform oscillations in space and periodic oscillations in time with the frequency

$$\omega_H = \mathrm{Im}(\lambda(k)) = \sqrt{\Delta_0} = \frac{\beta A\Big(\gamma(\alpha - 1) + A\Big)}{\gamma(\alpha - 1)}, \tag{8}$$

and the corresponding wavelength is

$$\lambda_H = \frac{2\pi}{\omega_H} = \frac{2\gamma(\alpha - 1)\pi}{\beta A(\gamma(\alpha - 1) + A)}. \tag{9}$$

The Turing instability is dependent not upon the geometry of the system but only upon the reaction rates and diffusion. And it cannot be expected when the diffusion term is absent and it can occur only when the activator (for predator-prey system, prey) diffuses more slowly than the inhibitor (for predator-prey system, predator). Mathematically speaking, as $d_1 \ll d_2$, the Turing bifurcation occurs when $\mathrm{Im}(\lambda(k)) = 0$ and $\mathrm{Re}(\lambda(k)) = 0$ at $k = k_T \neq 0$,

k_T is called the wavenumber. The critical value of bifurcation parameter γ equals

$$\gamma_T = \frac{A(\beta A+2d_2k_T^2+d_2Ak_T^2)}{(1-a)(\beta A+d_2k_T^2+d_2Ak_T^2-d_1d_2k_T^4)}, \tag{10}$$

where

$$k_T^2 = \sqrt{\frac{\Delta_0}{d_1d_2}}.$$

And at the Turing threshold, the spatial symmetry of the system is broken and the patterns are stationary in time and oscillatory in space with the wavelength

$$\lambda_T = \frac{2\pi}{k_T} = \frac{2\pi\sqrt[4]{d_1d_2\gamma^2(\alpha-1)^2}}{\sqrt{\beta A(\gamma(a-1)+A)}}. \tag{11}$$

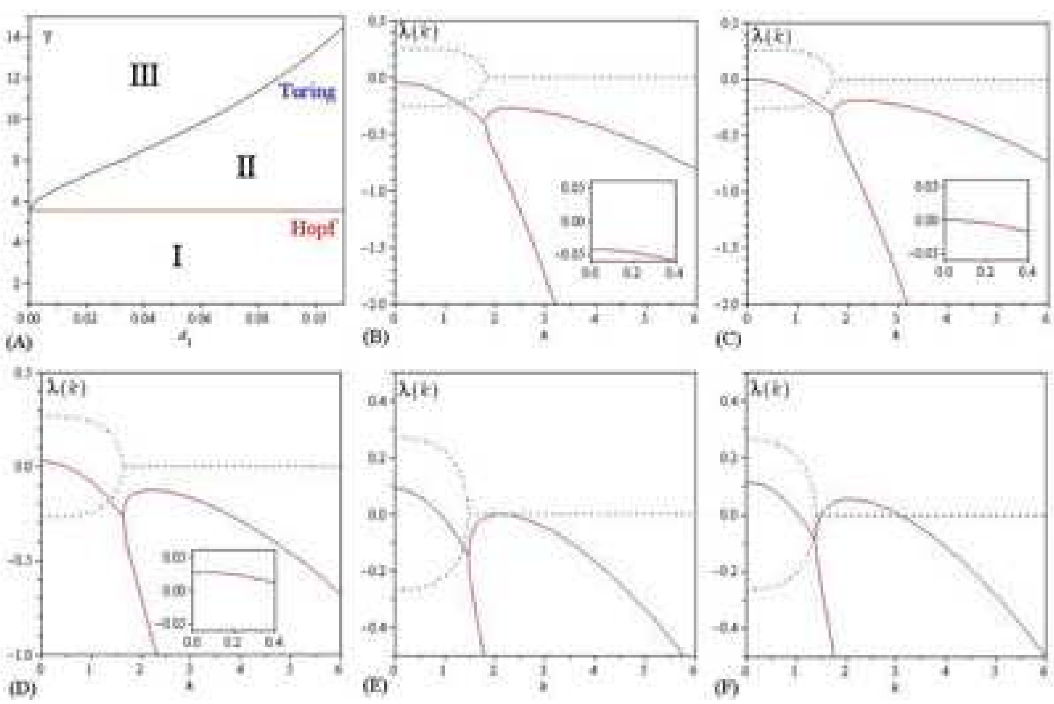

Fig. 1. (A) $\gamma - d_1$ Bifurcation diagram for the system (4) with $\alpha = 1.1$, $\beta = 0.5$, $d_2 = 0.2$. Hopf and Turing bifurcation lines separate the parameter space into three domains. The other parameters in figures (B)–(F): d_1=0.02, and (B) $\gamma = 5.0$; (C) $\gamma = 5.552147102$, the critical value of γ_H; (D) $\gamma = 6.0$; (E) $\gamma = 7.265163898$, the critical value of γ_T; (F) $\gamma = 8.0$. The real and the imaginary parts of $\lambda(k)$ are shown by solid lines and dotted lines, respectively.

Linear stability analysis of model (4) yields the bifurcation diagram, the relation between γ and d_1, is shown in figure 1(A). In this case, the Hopf bifurcation line and the Turing bifurcation line separate the parametric space into three distinct domains. In domain I, located below all Hopf and Turing bifurcation lines, the steady state is the only stable solution of the system. Domain II is the region of pure Hopf instability, and in domain III, located above all two bifurcation lines, both Hopf and Turing instability occur.

From the definition of Hopf and Turing bifurcation, we know that the relation between the real, the imaginary parts of the eigenvalue $\lambda(k)$ determine the bifurcation type. The relation between $\mathrm{Re}(\lambda(k))$, $\mathrm{Im}(\lambda(k))$ and k are shown in figure 1(B)–(F). Figure 1(B) illustrate the case of parameter locate in domain I in figure 1(A), $\gamma = 5.0$, one can see that $\mathrm{Re}(\lambda(k)) < 0$ and $\mathrm{Im}(\lambda(k)) \neq 0$ at $k = 0$. Figure 1(C), $\gamma = 5.552147102 \equiv \gamma_H$, the critical value of Hopf bifurcation, in this case, $\mathrm{Re}(\lambda(k)) = 0$ at $k = 0$ while $\mathrm{Im}(\lambda(k)) \neq 0$. In figure 1(D), $\gamma = 6.0$, the parameter locate in domain II, the pure Hopf instability occurs, one can see that at $k = 0$, $\mathrm{Re}(\lambda(k)) > 0$, $\mathrm{Im}(\lambda(k)) \neq 0$. Figure 1(E), $\gamma = 7.265163898 \equiv \gamma_T$, the critical value of Turing bifurcation, at $k = k_T = 2.116874108$, $\mathrm{Re}(\lambda(k)) = \mathrm{Im}(\lambda(k)) = 0$. When $\gamma = 8.0$, parameter locate in domain III, figure 1(F) indicate that at $k = 0$, $\mathrm{Re}(\lambda(k)) > 0$, $\mathrm{Im}(\lambda(k)) \neq 0$.

3 Pattern formation analysis

In this section, we have performed extensive numerical simulations of the spatially extended model (4) in two-dimensional space, and the qualitative results are shown here. Model (4) is posed on a given domain $\Omega = 400 \times 400$, with smooth boundary $\partial\Omega$. Zero-flux Neumann boundary conditions are imposed on $\partial\Omega$ to close the system. Model (4) is solved numerically with $\alpha = 1.1$, $\beta = 0.5$, $d_1 = 0.02$, $d_2 = 0.2$ in two-dimensional space using a finite difference approximation for the spatial derivatives and an explicit Euler method for the time integration (Garvie, 2007) with a time stepsize of $\Delta t = 1/3$ and space stepsize $\Delta h = 1/24$. We start with the unstable uniform solution (u^*, v^*) with small random perturbation superimposed. Thus the initial profiles of u and v are completely random without any spatial correlation. And we perform a series of of two-dimensional simulations (figures 2, 3 and 4), in each, the initial condition was always a small amplitude random perturbation ($\pm 5 \times 10^{-4}$) around the steady state (u^*, v^*), and patterns developed spontaneously.

In the numerical simulations, different types of dynamics are observed and we have found that the distributions of predator and prey are always of the same type. Consequently, we can restrict our analysis of pattern formation to one distribution. In this section, we show the distribution of prey, for instance.

From the analysis in section 2 and the bifurcation diagram (figure 1(A)), the results of numerical simulations show that when parameters α, β, d_2 are determined, the type of the system dynamics is determined by the values of γ and d_1. And for different sets of parameters, the features of the spatial patterns become essentially different when γ exceeds the critical value γ_H and γ_T respectively, which depend on d_1.

Figure 2 shows the evolution of the spatial pattern of prey at $0, 10000, 20000$

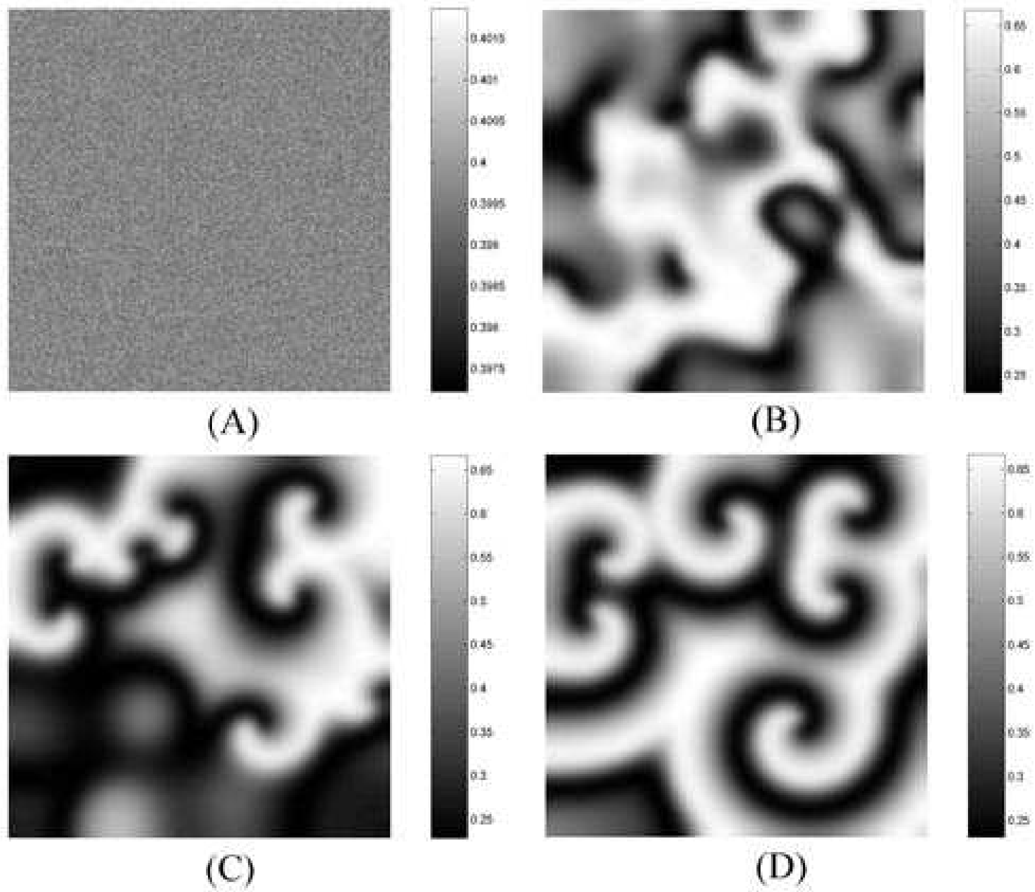

Fig. 2. Grey-scaled snapshots of contour pictures of the time evolution of the prey of model (4) with $\gamma = 6.0 > \gamma_H$. (A) 0 iteration; (B) 10000 iteration; (C) 20000 iteration; (D) 50000 iteration.

and 50000 iterations with $\gamma = 6.0$, more than the Hopf bifurcation threshold $\gamma_H = 5.552147102$ and less than the Turing bifurcation threshold $\gamma_T = 7.265163898$. In this case, one can see that for model (4), the random initial distribution around the steady state $(u^*, v^*) = (0.39965, 0.26392)$ leads to the formation of the spiral wave pattern in the domain (figure 2(D)). In other words, in this situation, spatially uniform steady-state predator-prey coexistence is no longer. Small random fluctuations will be strongly amplified by diffusion, leading to nonuniform population distributions. From the analysis in section 2, we find with these parameters in domain II, the spiral pattern arises from Hopf instability.

When $\gamma = 8.0 > \gamma_T = 7.265163898$, in this case, parameters in domain III (figure 1(A)), both Hopf and Turing instabilities occur. The nontrivial stationary state is $(u^*, v^*) = (0.29974, 0.23088)$. As an example, the formation of a regular macroscopic two-dimensional spatial pattern, the chaotic spiral pattern, is shown in figure 3.

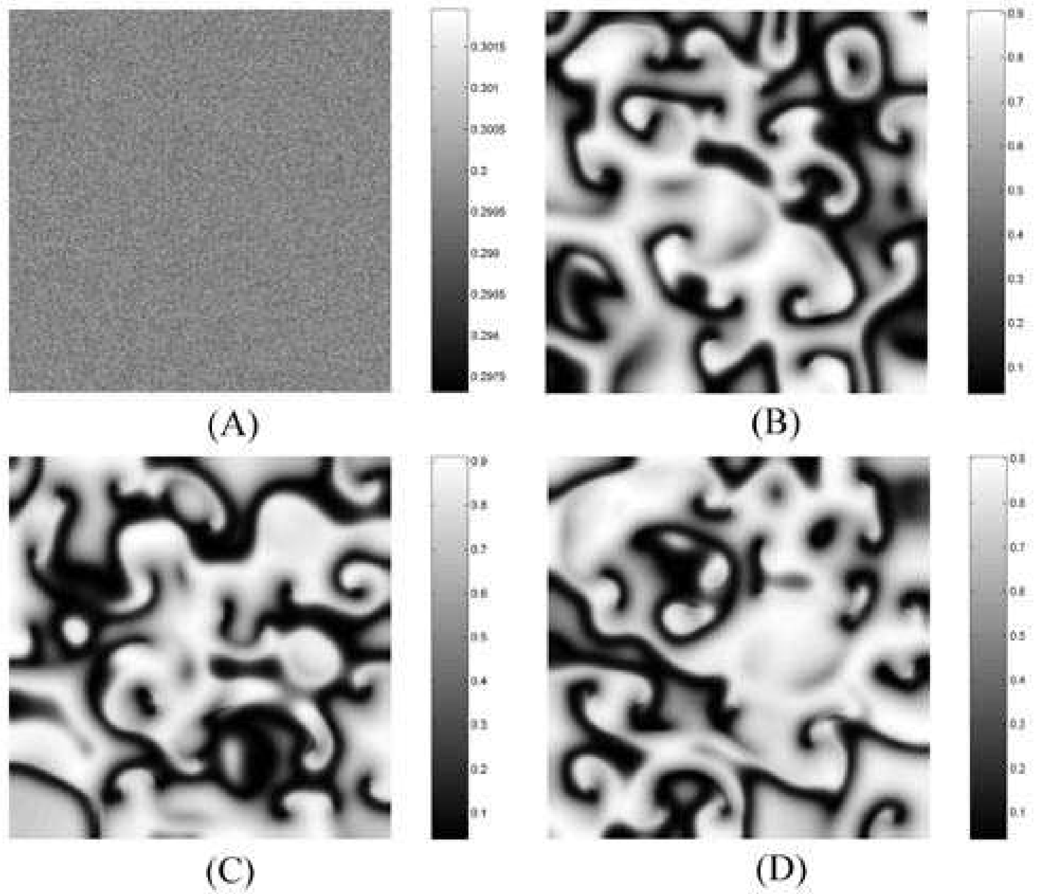

Fig. 3. Grey-scaled snapshots of contour pictures of the time evolution of the prey of model (4) with $\gamma = 8.0 > \gamma_T$. (A) 0 iteration; (B) 10000 iteration; (C) 20000 iteration; (D) 50000 iteration.

Comparing this situation (figure 3) with the one above (figure 2), we can see that the formation of chaotic spiral patterns (figure 3(C, D)) are caused by Turing instability.

For the sake of learning the dynamics of model (4) further, we illustrate the phase portraits and time-series plots in figure 4. From figure 4(A), for $\gamma = 6.0$, one can see that a quasi limit cycle arises, which is caused by the Hopf bifurcation. Furthermore, we can calculate that the frequency of periodic oscillations in time (figure 4(B)) is $\omega = 27.5899$, and corresponding wavelength $\lambda = 0.2277$. And from (8) and (9), we know that at the critical value of Hopf bifurcation γ_H, the frequency of the periodic oscillations in time is $\omega_H = 24.0748$, the corresponding wavelength $\lambda_H = 0.2610$. When $\gamma = 8.0$, the dynamical behavior are shown in figures 4(C) and (D). From figure 4(C), one can see that there exhibits a "local" phase plane of the system invaded by the irregular spatiotemporal oscillations. Instead of the limit cycle in the case above (figure 4(A)), as happens in the case of smooth pattern formation, the trajectory now fills nearly the whole domain inside the limit cycle. This regime of the

system dynamics corresponds to spatiotemporal chaos. And the spatial symmetry of model (4) is broken and the patterns are oscillatory in space with the wavelength $\lambda = 0.1629$ while at the critical value of Turing bifurcation, $\lambda_T = 0.2834$.

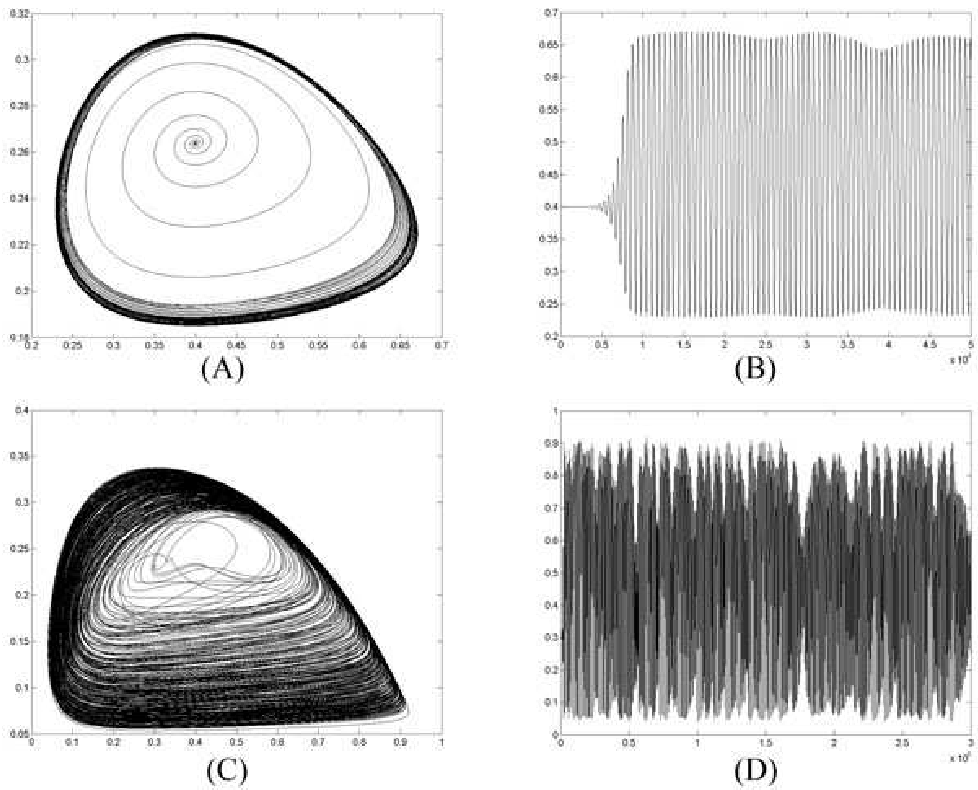

Fig. 4. Dynamical behavior of model (4). Phase planes of the model at a fixed point inside the domain occupied by irregular spatiotemporal oscillations with $\gamma = 6$ (A) and $\gamma = 8$ (C), respectively. Time-series plots with $\gamma = 6$ (B) and $\gamma = 8$ (D), respectively.

The above results are obtained from the initial conditions which was always a small amplitude random perturbation around the steady state (u^*, v^*). In references (Medvinsky et al, 2002; Sherratt, Eagan & Lewis, 1997; Garvie, 2007), the authors have studied the pattern formation arising from special initial conditions. They indicated that the spatiotemporal dynamics of a diffusion-reaction system depends on the choice of initial conditions. And the initial conditions are deliberately chosen to be asymmetric in order to make any influence of the corners of the domain more visible (Medvinsky et al, 2002). The initial localized introduction of predators into a uniform distribution of prey led to the spread of predators over the domain (Garvie, 2007). An important new feature in the two-dimensional solutions is the way in which asymmetries in the initial introduction of predators are reflected in the long-time solutions.

Based on the discussion above, we employ three categories of initial perturba-

tions (figure 5) for further learning the evolution of the spatial pattern of prey of model (4). In both parts of figure 5, predators were initially introduced in a spatially asymmetric manner. In the following, model (4) was solved numerically with a time stepsize of $\Delta t = 1$ and space stepsize $\Delta h = 1/3$.

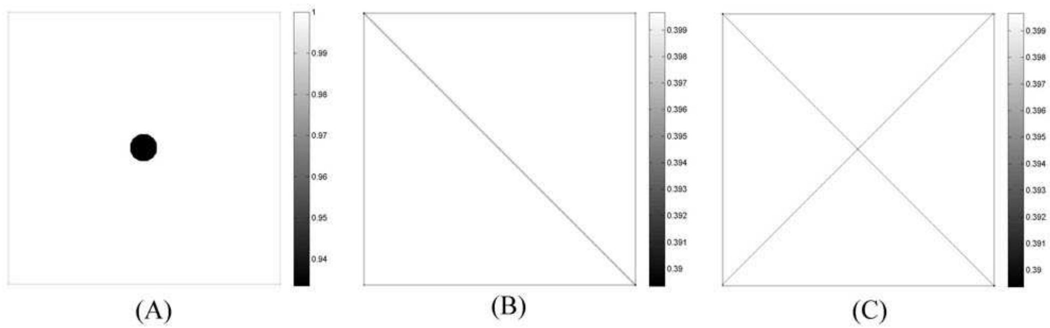

Fig. 5. Three categories of initial perturbations corresponding with figures 6—9.

In the first, predators are introduced in a small, localized region of the circle domain (Figure 5(A)):

$$\begin{aligned} u(x,y,0) &= 1.0, \\ v(x,y,0) &= \begin{cases} 0.2 & (x-200)^2+(y-200)^2<400, \\ 0 & otherwise \end{cases} \end{aligned} \tag{12}$$

The second category of initial perturbation that we have used is the introduction of predators along a line, which is otherwise in the steady state (u^*, v^*) (figure 5(B)):

$$\begin{aligned} u(x,y,0) &= u^* + 0.005 \cdot \exp\Big(-(x-200)^2-(y-200)^2\Big), \\ v(x,y,0) &= v^* - 0.005 \cdot \exp\Big(-|x-y|\Big). \end{aligned} \tag{13}$$

Thirdly, we employ the so-called pitchfork initial conditions (figure 5(C)):

$$\begin{aligned} u(x,y,0) &= u^* + 0.005 \cdot \exp\Big(-(x-200)^2-(y-200)^2\Big), \\ v(x,y,0) &= v^* - 0.005 \cdot \exp\Big(-\sqrt{|(x-y)(x+y-400)|}\Big). \end{aligned} \tag{14}$$

The numerical simulations results of pattern formation of model (4) with above three categories of initial perturbations are shown in figures 6 ($\gamma = 6.0$) and 7 ($\gamma = 8.0$).

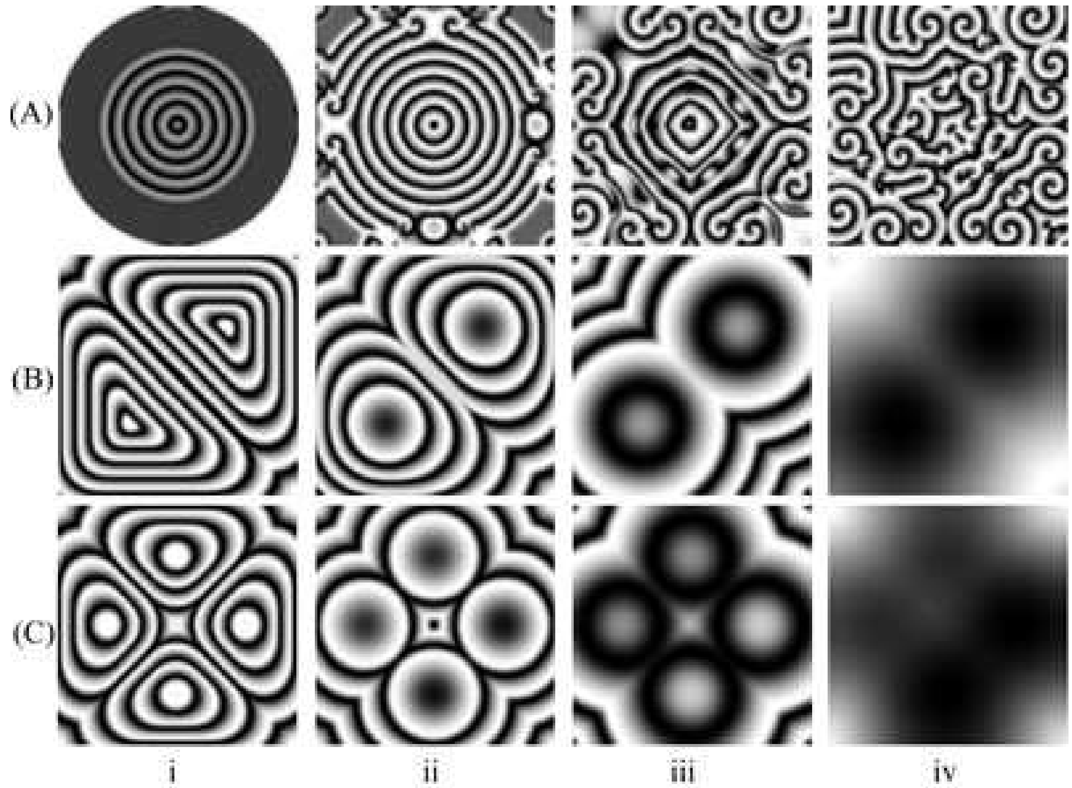

Fig. 6. Grey-scaled snapshots of contour pictures of the time evolution of the prey of system (4) at different instants with $\gamma_H < \gamma = 6.0 < \gamma_T$. (A)(B)(C) are the three category of initial conditions corresponding to Figure (4) and the iterations are: (i) 3000; (ii) 5000; (iii) 10000; (iv) 50000.

In figure 6(A), in the case of the first category of initial perturbation which predators are introduced in a small and localized region of the circle domain, one can see that after a symmetrical target pattern (figure 6(A)(i)), it grows slightly and the spiral pattern (exterior) with target pattern (interior) emerges (figure 6(A)(ii, iii)), finally with the appearance of spiral pattern in the whole domain (figure 6(A)(iv)). And in figure 7(A), $\gamma = 8.0$, with the same initial conditions, a target pattern (figure 7(A)(i)) emerges, the destruction of the target begins from the center, and leads to the formation of the spiral pattern (interior) with target pattern (exterior) (figure 7(A)(ii, iii)), finally, the chaotic spatial pattern prevails the whole domain (figure 7(A)(iv)). Comparing Figure 6(A)(iv) with figure 7(A)(iv), we find that Hopf instability leads to the formation of spiral patterns and the Turing instability destroys the spiral pattern and leads to the formation of chaotic spatial patterns. Moreover, in these two cases, the initial nonuniformity spreading outwards through the domain from the center provides additional evidence for spatiotemporal pattern.

In figure 6(B), with initial condition (13), bi-target pattern (figure 6(B)(i)) emerges, and finally, the phase waves appear in the whole domain (figure 6(B)(iv)). And in figure 7(B), more differently, after a target pattern(figure 7(B)

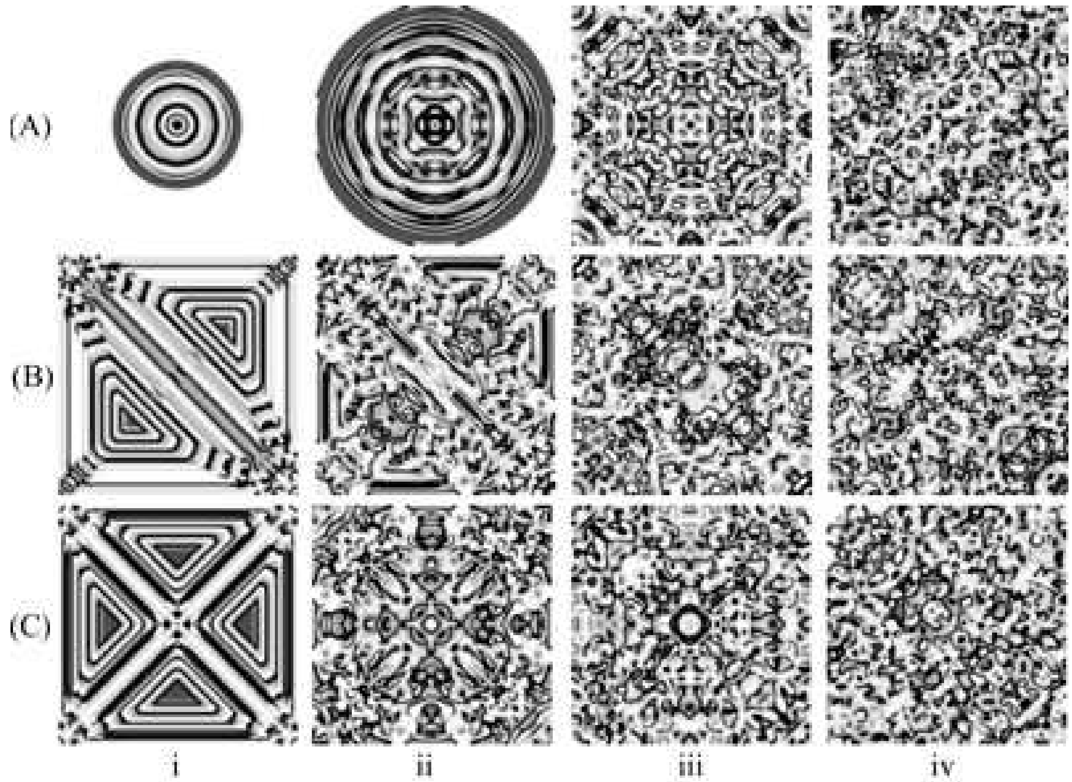

Fig. 7. Grey-scaled snapshots of contour pictures of the time evolution of the prey of system (4) at different instants with $\gamma = 8.0 > \gamma_T$. (A)(B) (i) 1500; (ii) 3000; (iii) 5000; (iv) 50000. (C) (i) 1000; (ii) 3000; (iii) 5000; (iv) 50000.

(i)), a chaotic spatial pattern occurs (figure 7(B)(iii, iv)).

In the case of the third category initial perturbation (14), one can see that figure 6(C) and 7(C) follow similar scenario to the previous case, respectively (figures 6(B) and 7(B)). The differences are that there are four-target patterns (figure 6(C)(i) and 6(C)(ii)) while in the previous case bi-target patterns occur. Comparing these two cases with the initial perturbations defined by equations (13) and (14), we find that in the beginning of evolution of the spatial pattern of prey, the special initial conditions have an effect on the formation of spatial patterns, though the effect is less and less with the more and more iterations.

In order to make it more clearer, we show space-time plots in figures 8($\gamma = 6.0$) and 9($\gamma = 8.0$). The method of space-time plots is that let y be a constant (here, $y = 200$, the center line of each snapshots), from each pattern snapshots, choose the line $y = 200$, and pile these lines in-time-order. The space-time plots show the evolution process of the prey u throughout time t and space x. On the other hand, we have found that the distributions of predator and prey are always of the same type. In this section, we show the distribution of prey, for instance.

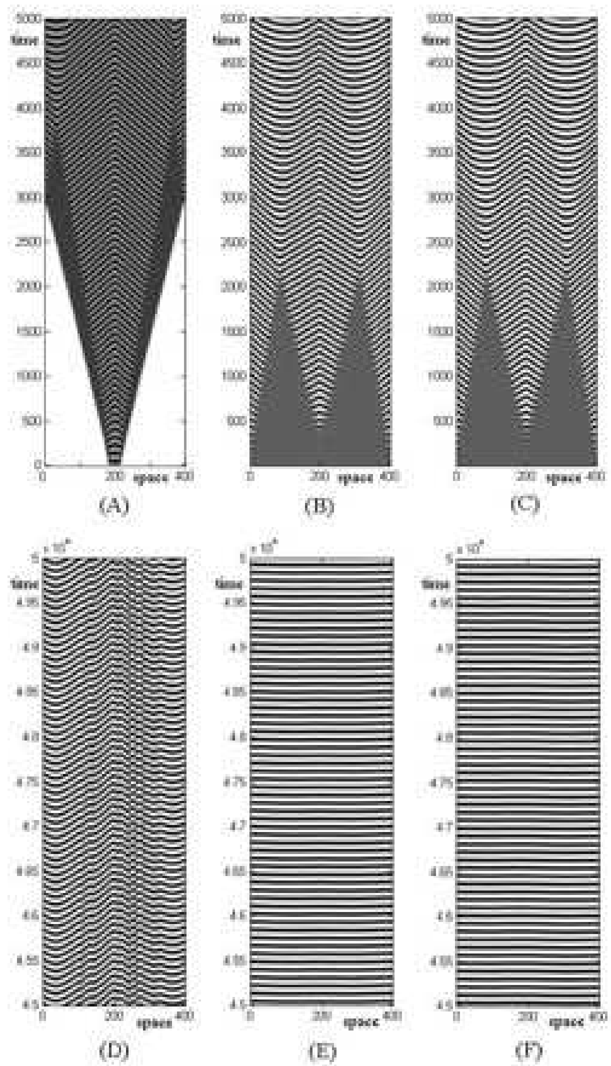

Fig. 8. Space-time plots of variable $\gamma = 6.0$. Other parameters are the same as those in Figure2 and 6.

In figure 8, $\gamma = 6.0$, other parameters equal figures 2 and 6, with the three categories of initial perturbations (figure 5), space-time plots at different times are shown. The first row in figure 8(A–C) displays the time evolution of the prey with the iterations from 0 to 5000, while the second row (figure 8(D–F)) displays the time evolution of the prey with the iterations from 45000 to 50000. The three columns correspond to the three categories of initial perturbations (figure 5). Form figure 8 and figure 6, one can see that when $\gamma = 6.0$, in this case, the Hopf instability occurs, the circular initial condition creates spiral wave (figure 6(A) and figure 8(D)), and the other two initial conditions create phase wave (figure 6(B, C) and figure 8(E, F)). Furthermore, in this case, the second and third initial conditions have the same effect on pattern formation (figure 8(E, F)).

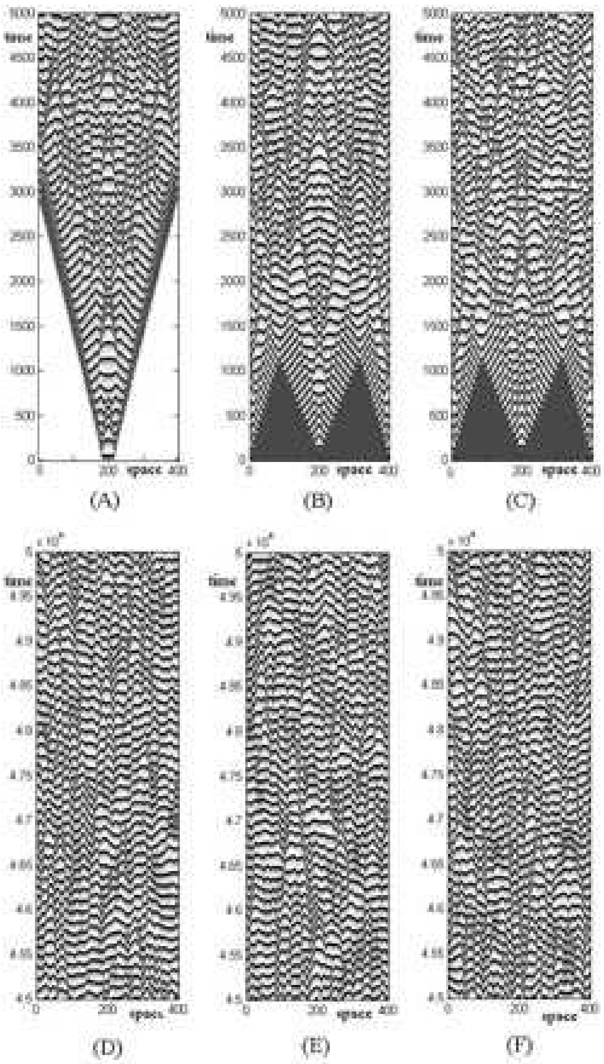

Fig. 9. Space-time plots of variable $\gamma = 8.0$. Other parameters are the same as those in Figure 3 and 7.

When $\gamma = 8.0$, other parameters equal figures 3 and 7, space-time plots at different times with the three categories of initial perturbations (figure 5) are shown in figure 9. In this case, both Hopf and Turing instability occur. Figure 9(A–C), displays the time evolution of the prey with the iterations from 0 to 5000, while the second row (figure 9(D–F)) displays the time evolution of the prey with the iterations from 45000 to 50000. The three columns correspond to the three categories of initial perturbations (figure 5). Form figure 9 and figure 7, one can see that all three initial conditions have the same effect on pattern formation (figure 7(iv) and figure 9(D–F)).

In our previous work (Wang, Liu & Jin, 2007), we indicated that for the ratio-dependent predator-prey system with Michaelis-Menten-type functional response, the case of predator-dependent, the stationary patterns did not depen-

dent on the initial conditions. One can see that, in the case of prey-dependent type (4), pattern formation do depend on the initial conditions. This is a major difference between prey-dependent and predator-dependent predator-prey models.

4 Discussions

In this paper, we have presented a theoretical analysis of evolutionary processes that involve organisms distribution and their interaction of spatially distributed population with local diffusion. And the numerical simulations were consistent with the predictions drawn from the bifurcation analysis, that is, Hopf bifurcation and Turing bifurcation.

If the parameter γ in the domain II, the Hopf instability occurs, the destruction of the pattern begins from the interior, while it begins from the exterior if γ located in the domain III, both Hopf and Turing instabilities occur. From an ecological viewpoint (Sherratt, Eagan & Lewis, 1997), it shows that the initial and relatively rapid invasion of prey by predators can be followed by two subsequent invasions.

The effort to explain the distribution of populations in terms of the movements of individuals is an extension of one of the most successful applications of mathematics to ecological phenomena, the use of diffusion model to describe dispersal. The basic idea is that, although organisms do not move randomly, the collective behavior of large numbers of such individuals may be indistinguishable (at the scale of the population) from what they did (Levin, 1992). In references (Levin, 1992; Savill & Hogeweg, 1999; Alonso, Bartumeus & Catalan, 2002), the authors indicated that the basic idea of diffusion-driven instability in a reaction-diffusion system can be understood in terms of an activator-inhibitor system. The functioning of this mechanism is based on three points (Alonso, Bartumeus & Cat 2002). First, a random increase of activator species should have a positive effect on the creation rate of both activator and inhibitor species. Second, an increment in inhibitor species should have a negative effect on formation rate of both species. Finally, inhibitor species must diffuse faster than activator species. Certainly, the reaction-diffusion predator-prey model (4), with Ivlev functional response and predators diffusing faster than prey, provides this mechanism.

Spirals and curves are the most fascinating clusters to emerge from the predator-prey model. A spiral will form from a wave front when the rabbit line (which is leading the front) overlaps the pursuing line of predator. The prey on the extreme end of the line stop moving as there are no predator in their immediate vicinity. However the prey and the predator in the center of the line continue

moving forward. This forms a small trail of prey at one (or both) ends of the front. These prey start breeding and the trailing line of prey thickens and attracts the attention of predator at the end of the fox line that turn towards this new source of prey. Thus a spiral forms with predator on the inside and prey on the outside. If the original overlap of prey occurs at both ends of the line a double spiral will form. Spirals can also form as a prey blob collapses after predator eat into it (Hawick, James & Scogings, 2006).

And a random increase of activator species (prey, u) has a positive effect on the creation rate of both activator and inhibitor species. Random fluctuations may cause a nonuniform prey density. This elevated prey density has a positive effect both on prey and predator population growth rates. From model (3), we can obtain per capita rates:

$$\frac{1}{u}\frac{\partial u}{\partial t} = (1-u) - \frac{v}{u}(1-e^{-\gamma u}), \qquad \frac{1}{v}\frac{\partial v}{\partial t} = \beta(\alpha - 1 - \alpha e^{-\gamma u}). \tag{15}$$

Since the first equation in (15) is a one-humped function of prey density u, prey growth rate can be increased by a higher local prey density at least in a range of parameter values. The second equation in (15), predator numerical response, is an ever-increasing function of u, and high prey density always has a positive influence on predator growth. More importantly, inhibitor species (predator, v) must diffuse faster than activator species (prey, u), for an increment in inhibitor species may have a negative effect on formation rate of both species. Thus, as random fluctuations increase local prey density over its equilibrium value, prey population undergoes an accelerated growth. Simultaneously, predator population also increases, but as predators diffuse faster than prey, they disperse away from the center of prey outbreaks. If relative diffusion (d_2/d_1) is large enough, prey growth rate will reach negative values and prey population will be driven by predators to a very low level in those regions. In other words, where the prey density is at their maximal value diffusion will lower the prey density at that point. Conversely, where the prey density is at their minimal value diffusion will increase the prey density at that point. That is, prey flow from high density to low density regions in space. Moreover, the faster the diffusion the greater the flow. When the prey density is high (in fact, when $\nabla^2 u < 0$) proportionately less of the slower diffusing prey leaves these points in space than the faster diffusion prey and, therefore, the proportion of the slower diffusing prey at that point increases more than the proportion of the faster diffusing prey. Conversely, at low prey density (when $\nabla^2 u > 0$) proportionately more faster diffusing prey enter a point in space and the proportion of these prey increases more than the proportion of the slower diffusing prey. Hence, at a given position in space, when the prey density is high the proportion of slower diffusing prey increases and when the prey density is low the proportion of the faster diffusing prey increases. There-

fore we see oscillations in the proportions of the prey at the same frequency as the oscillations of the density waves. The final result is the formation of patches of high prey density is surrounded by areas of low prey density. And predators follow the same pattern.

On the other hand, in two-dimensional reaction-diffusion systems, rotationally symmetric patterns, known as targets or sinks, and a generalization of them with broken circular symmetry, spirals are being investigated experimentally as well as theoretically in many nonlinear systems. The Belousov-Zabotinsky reaction is a well investigated excitable reaction-diffusion system that shows all these patterns. Spirals are characteristic patterns in slime mold aggregates and are an important observation in cardiac arrythmias as well. Targets and spirals, which are generally found to form around some defects, precede some defect mediated chaos, commonly known as spiral defect chaos (Bhattacharyay, 2001).

Particularly, spiral patterns are being investigated theoretically in a number of reaction-diffusion predator-prey systems, such as Holling-type model (Savill & Hogeweg, 1999; Malchow et al, 2000), Ivlev-type (Sherratt, Lewis & Fowler, 1995; Sherratt, Eagan & Lewis, 1997; Kay & Sherratt, 2000; Pearce et al, 2006; Garvie, 2007; Preedy et al., 2006; Uriu & Iwasa, 2007), and so on. The functional responses of these predator-prey models are all prey-dependent. It is necessary or coincident?

It is well known that, for reaction-diffusion predator-prey systems, under suitable conditions, the destabilized uniform distributions give way to stable nonuniform patterns, which can provide the local information of that specifies patterns of differentiation (Levin, 1992). In reference (Alonso, Bartumeus & Catalan, 2002), the authors also indicted that a simple general model for predator-prey dynamics with predator-dependent functional response, a reaction-diffusion system that could develop diffusion-driven instabilities. On the contrary, if the functional response depends only on prey density, diffusion instabilities are not possible. In fact, in the case of predator-dependent, the interactions between dispersing populations induce spatial heterogeneity and/or temporal fluctuations through so-called self-structuring without help from external forcing, and the patterns are endogenous. While the prey-dependent predator-prey models are self-oscillation ones which are called oscillatory systems, there are typical patterns including spiral waves, turbulence, and target patterns. This is the reason why we can find the spiral and target waves in model (4).

From the theoretical study on the three-dimensional patterns (Leppänen et al, 2003; Leppänen, 2004), it is possible that the three-dimensional patterns can be reflected by the two-dimensional patterns. And two-dimensional patterns might be sufficient to understand the general properties of dissipative structures (Shoji, Yamada, Ueyama & Ohta, 2007). So our two-dimensional spatial patterns may indicate the vital role of pattern formation in the three-

dimensional spatiotemporal organization of the predator-prey system.

Furthermore, from references (Sherratt, Perumpanani & Owen, 1999; Byrne et al, 2006), we think that pattern formation of spatial model (4) with special choice initial conditions (12)–(14) can be used to explain other diffusion process, such as tumor growth, and so on.

On the other hand, the ecosystem is so complicated that we cannot use a single method to study. We must use mixed methods, such as analytical or experimental or numerical method.

Acknowledgments

This work is by the Knowledge Innovation Project of the Chinese Academy of Sciences (KZCX2-YW-430), the National Basic Research Program (2006CB403207) and the Youth Science Foundation of Shanxi Provence (20041004).

References

Abrams P., and Ginzburg L., 2000. The nature of predation: prey dependent, ratio dependent or neither? Trends Ecol. Evol. 15, 337-341.

Alonso, D., Bartumeus, F., Catalan, J., 2002. Mutual interference between predators can give rise to Turing spatial patterns, Ecology 83, 28-34.

Arditi R., and Ginzburg L., 1989. Coupling in predator-prey dynamics: Ratio-dependence, J. Theor. Biol. 139, 311-326.

Baurmann, M., Gross, T., Feudel, U., 2007, Instabilities in spatially extended predator-prey systems: Spatio-temporal patterns in the neighborhood of Turing-Hopf bifurcations, J. Theo. Biol. 245, 220-229.

Beddington, J., 1975. Mutual interference between parasites or predators and its effect on searching efficiency, J. Anim. Ecol. 44, 331C340.

Ben-Jacob, E., Levine, H., 2001. The artistry of nature, Nature, 409, 985-986.

Bhattacharyay, A., 2001. Spirals and targets in reaction-diffusion systems, Phys. Rev. E. 64, 016113(4).

Byrne, H. M., Alarcon, T., Owen, M. R., Webb, S. D., and Maini, P. K., 2006. Modelling aspects of cancer dynamics: a review, Phil. Trans. R. Soc. A, 364, 1563-1578.

Callahan, T., Knobloch, E., 1999. Pattern formation in the three-dimensional reaction-diffusion systems, Phys. D 132, 339-362.

Cantrell, R., and Cosner, C., 2003. Spatial Ecology via Reaction-Diffusion Equations, John Wiley & Sons, Ltd., Chichester, England.

Crowley P., Martin E., 1989. Functional responses and interference within and between year classes of a dragonfly population, J. North Amer. Bent. Soc., 8, 211-221.

DeAngelis D., Goldstein R., and Neill R., A model for trophic interaction, Ecology 56, 881-892.

Garvie, M., 2007. Finite-difference schemes for reaction-diffusion equations modelling predator-prey interactions in matlab, Bull. Math. Biol. 69, 931-956.

Griffith, D., Peres-Netob, P., 2006. Spatial modeling in ecology: the flexibility of eigenfunction spatial analyses, Ecology 87, 2603-2613.

Hassell M., and Varley C., 1969. New inductive population model for insect parasites and its bearing on biological control, Nature 223, 1133-1177.

Hawick, K., James, H., Scogings, C., 2006. A zoology of emergent life patterns in a predator-prey simulation model, Technical Note CSTN-015 and in Proc. IASTED International Conference on Modelling, Simulation and Optimization, September 2006, Gabarone, Botswana. 507-115.

Holling C., 1959. The components of predation as revealed by a study of small mammal predation of the european pine sawfly, Cana. Ento. 91, 293-320.

Holling C., 1959. Some characteristics of simple types of predation and parasitism, Cana. Ento. 91, 385-395.

Ivlev, V., 1961. Experimental ecology of the feeding fishes, Yale University Press, New Haven.

Jost, C., 1998. Comparing predator-prey models qualitatively and quantitatively with ecological time-series data, PhD-Thesis, Institute National Agronomique, Paris-Grignon.

Kay, A., Sherratt, J., 2000. Spatial noise stabilizes periodic wave patterns in oscillatory systems on finite domains, SIAM J. Appl. Math. 61, 1013-1041.

Koch, A., Meinhardt, H., 1994. Biological pattern formation: from basic mechanisms to complex structures, Revi. Mode. Phys. 66, 1281-1507.

Kooij, R., 1996. A predator-prey model with Ivlev's functional response, J. Math. Anal. Appl. 198, 473-489.

Kuang Y., Beretta E., 1998. Global qualitative analysis of a ratio-dependent predator-prey system, J. Math. Biol. 36, 389-406.

Leppänen, T., 2004. Coputational studies of pattern formation in turing systems, Phd-thesis, Helsinki University of Technology, Finland.

Leppänen, T., Karttunen, M., Kaski, K., Barrio, R., 2003. Dimensionality effects in turing pattern formation, Inter. J. of Mod. Phys. B 17, 5541-5553.

Levin, S., 1992. The Problem of Pattern and Scale in Ecology, Ecology 73, 1943-1967.

Liu, Q.-X., Jin, Z., 2007. Formation of spatial patterns in epidemic model with constant removal rate of the infectives, J. Stat. Mech. P05002.

Malchow, H., Radtke, B., Kallache, M., Medvinsky, A., Tikhonov, D. , Petrovskii, S., 2000. Spatio-temporal pattern formation in coupled models of plankton dynamics and fish school motion. Nonl. Anal.: Real World Appl. 1, 53-67.

Maini, P., Baker, R., Chuong, C., 2006. The Turing model comes of molecular age, Science 314, 1397-1398.

May, R., 1981. Stability and complexity in model ecosystems. Princeton University Press, American.

Medvinsky A., Petrovskii S., Tikhonova I., Malchow H., Li B-L., 2002. Spatiotemporal complexity of plankton and fish dynamics, SIAM Review 44, 311-370.

Metz, J., Diekmann, O. 1986. A gentle introduction to structured population models: three worked examples. In: The dynamics of ph.siologicall. structured populations (Lecture Notes in Biomathematics 68) (ed. Metz, J., Diekmann,O.), pp. 3-45. Berlin: Springer.

Murray, J., 2003. Mathematical Biology II: Spatial Models and Biomedical Applications. Springer, Berlin.

Neuhauser, C., 2001. Mathematical challenges in spatial ecology, Noti. Amer. Math. Soc. 47, 1304-1314.

Pearce, I., Chaplain, M., Schofield, P., Anderson, A., Hubbard, S., 2006. Modelling the spatio-temporal dynamics of multi-species host-parasitoid interactions: Heterogeneous patterns and ecological implications, J. Theo. Biol. 241, 876-886.

Preedy, K., Schofield, P., Chaplain, M., Hubbard S., 2006. Disease induced dynamics in host-parasitoid systems: chaos and coexistence, J. R. Soc. Inte. doi:10.1098/rsif.2006.0184.

Ruan, S., Xiao, D., 2001. Global Analysis in a Predator-Prey System with Nonmonotonic Functional Response, SIAM J. Appl. Math. 61, 1445-1472.

Savill, N., Hogeweg, P., 1999. Competition and dispersal in predator-prey waves, Theo. Popu. Biol. 56, 243-263.

Schnell, S., Grima, R., Maini, P., 2007. Multiscale Modeling in Biology, Amer. Scie. 95, 134-142.

Sherratt, J., Lewis, M., Fowler, A., 1995. Ecological chaos in the wake of invasion, Proc. Nati. Acad. Sci. 92, 2524-2528.

Sherratt, J., Eagan, B., Lewis, M., 1997. Oscillations and chaos behind predatorcprey invasion: Mathematical artifact or ecological reality? Phil. trans. Roy. Soc. Lond.-B 352, 21-38.

Sherratt, J., Perumpanani, A., Owen, M., 1999. Pattern Formation in Cancer. In: On Growth and Form: Spatio-temporal Pattern Formation in Biology, (editors: M.A.J. Chaplain, G.D. Singh, J.C. McLachlan), John Wiley & Sons Ltd.

Shoji, H., Yamada, K., Ueyama, D., Ohta, T., 2007. Turing patterns in three dimensions, Phys. Revi. E 75, 046212(13).

Sugie, J., 1998. Two-parameter bifurcation in a predator-prey system of ivlev type, J. Math. Anal. & Appl. 217, 349-371.

Tian, R., 2006. Toward standard parameterization in marine biological modeling, Ecol. Model. 193, 363-386.

Turing, A., 1952. The chemical basis of morphogenesis. Phil. trans. Royal. Soc. Lond.-B 237 (B 641), 37-72.

Wang, H., Wang, W., 2007. The dynamical complexity of a Ivlev-type prey-predator system with impulsive effect, Chaos, Soli. Frac. DOI: 10.1016/j.chaos.2007.02.008.

Wang, W., Liu, Q.-X., Jin, Z., 2007. Spatiotemporal com plexity of a ratio-dependent predator-prey system, Phys. Rev. E 75, 051913.

Yang, L., Dolnik, M., Zhabotinsky, A., Epstein, I., 2002. Pattern formation arising from interactions between turing and wave instabilities, J. Chem. Phys. 117, 7259-7265.

Uriu K., Iwasa Y., 2007. Turing pattern formation with two kinds of cells and a diffusive chemical, Bull. Math. Biol. DOI: 10.1007/s11538-007-9230-0.